

A high temperature equation of state for the H₂O-CaCl₂ and H₂O-MgCl₂ systems

Zhenhao Duan ^{a,*}, Nancy Moller ^b, John H. Weare ^b

^a State Key Laboratory of Lithospheric Evolution, Institute of Geology and Geophysics, Chinese Academy of Sciences, Beijing 100029, China

^b Department of Chemistry and Biochemistry, 0340, University of California, San Diego, La Jolla, CA 92093, USA

Received 18 January 2006; accepted in revised form 17 May 2006

Abstract

An equation of state (EOS) is developed for salt-water systems in the high temperature range. As an example of the applications, this EOS is parameterized for the calculation of density, immiscibility, and the compositions of coexisting phases in the CaCl₂-H₂O and MgCl₂-H₂O systems from 523 to 973 K and from saturation pressure to 1500 bar. All available volumetric and phase equilibrium measurements of these binaries are well represented by this equation. This EOS is based on a Helmholtz free energy representation constructed from a reference system containing hard-sphere and polar contributions plus an empirical correction. For the temperature and pressure range in this study, the electrolyte solutes are assumed to be associated. The water molecules are modeled as hard spheres with point dipoles and the solute molecules, MgCl₂ and CaCl₂, as hard spheres with point quadrupoles. The free energy of the reference system is calculated from an analytical representation of the Helmholtz free energy of the hard-sphere contributions and perturbative estimates of the electrostatic contributions. The empirical correction used to account for deviations of the reference system predictions from measured data is based on a virial expansion. The formalism allows generalization to aqueous systems containing insoluble gases (CO₂, CH₄), alkali chlorides (NaCl, KCl), and alkaline earth chlorides (CaCl₂, MgCl₂). The program of this model is available as an electronic annex (see EA1 and EA2) and can also be downloaded at: <http://www.geochem-model.org/programs.htm>.

© 2006 Elsevier Inc. All rights reserved.

1. Introduction

Models of the thermodynamic behavior of fluid phases as a function of temperature (T), pressure (P), and composition (X) are essential for the quantitative analysis of geochemical processes. Of particular importance to the interpretation of systems containing aqueous solutions are the volumetric properties of the aqueous phase, the activity of the solute and solvent species in this phase and the PTX conditions under which homogeneous brine separates into two fluid phases of quite different compositions and mobility. The activities of water and solutes determine mineral stabilities (Gunter and Eugster, 1978; Henley et al., 1984; Brimhall and Crerar, 1987; Newton, 1995; Aranovich and Newton, 1997; Aranovich and Newton, 1998; Hauzen-

berger et al., 2001; Pak et al., 2003). The large changes in mobility and composition resulting from phase separation can have a great influence on processes such as the formation and alteration of mineral assemblages (Frantz et al., 1992; Newton et al., 1998), the evolution of geothermal fluids (Hass, 1971; Henley et al., 1984; Fournier, 1987), and the evolution of seafloor hydrothermal systems (Bischoff and Pitzer, 1985).

Experimental measurements provide the most reliable source of thermodynamic information for the interpretation of geochemical processes. However, the large amount of data required to describe the wide range of TPX conditions encountered in a typical application is often not available. In addition, for the high TP regions experienced in the deep crust or mantle, experimental measurements are difficult and the existing experimental data may not directly provide the thermodynamic information required for interpretation. For example, free energy is required for stability estimates, but for many conditions only PVTX data is

* Corresponding author.

E-mail address: duanzhenhao@yahoo.com (Z. Duan).

available. In order to generalize, interpolate, and extrapolate experimental data it is common to develop equations of state (EOS) representations (Carmichael and Eugster, 1987; Newton, 1995). Expressed as a function of temperature, pressure (or density), and composition, a well developed EOS can yield all thermodynamic properties (such as fugacity, free energy, phase equilibrium, and volumetric properties). For example, the pure system free energy EOS of Wagner and coworkers (Span and Wagner, 1996; Wagner and Pruß, 2002) summarizes the large amount of data available for pure systems in terms of a model Helmholtz free energy with accuracy equivalent to that of the measurements. With attention to the selection of the equation form and parameterization, an EOS can also provide highly accurate estimates of the thermodynamic properties of aqueous mixtures without salts (Duan et al., 1992). Many natural aqueous fluids contain high concentrations of dissolved salts dominated by the NaCl component. Accurate EOS for these systems have also been reported (Anderko and Pitzer, 1993a; Duan et al., 1995, 2003).

In many natural waters Ca and Mg chlorides are also found in high concentrations (White et al., 1963; Frapé and Fritz, 1987; Shvartsev and Bukaty, 1995) and the inclusion of these species in an EOS representation would be useful for geochemical interpretations. The thermodynamic properties of CaCl₂-H₂O and MgCl₂-H₂O have been studied extensively. Holmes et al. (1994) reported an EOS based on Pitzer equations (Pitzer, 1987; Weare, 1987) for liquid phases of the CaCl₂-H₂O system up to 523 K and 4.75 m. Pitzer and Oakes (1994) extended this model from 4.75 m to solid CaCl₂ saturation. Wang et al. (1998b) reported an EOS for MgCl₂-H₂O for T up to 623 K, also based on a Pitzer type model with virial coefficients up to fifth order. This model reproduces experimental data accurately below 523 K, but does not accurately predict water activities or vapor pressures for higher temperatures.

In this article, we present an EOS for the Helmholtz free energy EOS of the CaCl₂-H₂O and MgCl₂-H₂O binaries for high temperatures ($T > 523$ K). To improve the interpolation and extrapolation of the EOS, the free energy contributions are divided into those of a reference system based on a molecular level model and an empirical correction (Anderko and Pitzer, 1993a,b). As suggested by the interpretation of conductance data by Frantz and Marshall (1982), and solubility measurements by Gunter and Eugster (1978), we assume that solute species are fully associated for this high temperature range. In the reference system, the linear CaCl₂ and MgCl₂ molecules are approximated as hard spheres with point quadrupoles and the water molecules as hard spheres with point dipoles. A virial type empirical term is included in the EOS to correct for deviations between reference system predictions and measurements. This approach was previously used by Jiang and Pitzer (1995, 1996, JP model) for the CaCl₂-H₂O system. However, there are important differences in the mixing descriptions used in the model presented here and in that of Jiang and Pitzer. Therefore, a complete description of

the model is given in the next section and Appendix A. The models presented here will provide accurate predictions of volumetric and phase equilibrium properties for the CaCl₂-H₂O and MgCl₂-H₂O systems from 523 to 973 K and up to 1500 bar with possible extrapolation to higher temperatures and pressures. In addition, this EOS formalism allows generalization to systems containing NaCl, KCl, and insoluble gases.

2. The equation of state

The molar Helmholtz free energy, a , may be written as,

$$a(T, v, X) = a^{\text{res}}(T, v, X) + a^{\text{id}}(T, v, X), \quad (1)$$

where a^{res} and a^{id} are the residual and ideal gas molar Helmholtz free energies of the mixture and v is molar volume. The EOS developed here is based on the Helmholtz free energy. However, the application and parameterization of the EOS often involves volumetric or phase coexistence calculations. These properties can be obtained from derivatives of a . The compressibility factor, $Z = Pv/RT$, is given by,

$$Z = -v \left[\frac{\partial(a^{\text{res}}/RT)}{\partial v} \right]_T + 1, \quad (2)$$

and the partial molar fugacity coefficients by,

$$\ln \phi_i = \left[\frac{\partial(a^{\text{res}}/RT)}{\partial n_i} \right]_{v,T,n_{j \neq i}} - \ln Z + Z - 1, \quad (3)$$

where n_i is the number of moles of species i and n are the total number of moles in the phase. Equations for these properties using the EOS developed here are given in Appendix A.

To provide optimal interpolation and extrapolation of mixing properties, the functional form of the residual free energy should be based on a reasonably accurate molecular level description of the system. The thermodynamic perturbation theory originally introduced by Pople (1954) provides a framework from which such an EOS may be generated. This approach was developed by Stell, Rushbrooke and coworkers to treat polar systems (Stell et al., 1972, 1974; Rushbrooke et al., 1973). In these early applications, the qualitative behavior of polar fluids was analyzed in terms of the Helmholtz free energy of a system of hard spheres with point dipoles or quadrupoles representing polar interactions. The reference system included a hard-sphere contribution (hs) and electrostatic (es) dipole or quadrupole contributions to a^{res} ,

$$a^{\text{res}} = a^{\text{hs}} + a^{\text{es}}. \quad (4)$$

The hard-sphere contribution was provided by an analytical representation of simulation results (see below). Low order perturbation theory does not provide a very useful approximation to a^{es} . However, a quite accurate while still manageable approximation may be generated by a Padé approximation scheme (Stell et al., 1972, 1974; Rushbrooke et al., 1973). This level of the theory was successful-

ly applied to the qualitative analysis of polar fluid behavior by Gubbins and coworkers (Twu et al., 1975; Gubbins and Twu, 1978; Twu and Gubbins, 1978; Gubbins, 1985; Chapman et al., 1987). While the direct application of these methods can provide fairly accurate estimations of the thermodynamics of weakly polar solutions, their application to strongly polar and associated systems such as water is less satisfactory (Winkelmann, 1981, 1983). To provide the high level of accuracy necessary for the quantitative description of thermodynamic data, Prausnitz and coworkers (Bryan and Prausnitz, 1987; Dohrn and Prausnitz, 1990) added an empirical correction, a^{per} , to the EOS. The free energy now has a reference system made of hard-sphere atoms with dipole–dipole, dipole–quadrupole, and quadrupole–quadrupole interactions and an empirical contribution to account for inaccuracies calculation due to the inadequacy of the reference system.

$$a^{\text{res}} = a^{\text{ref}} + a^{\text{per}} = a^{\text{hs}} + a^{\text{es}} + a^{\text{per}}. \quad (5)$$

This EOS was shown to produce good predictions of associated fluids such as water by Bryan and Prausnitz (1987). Using this approach but with a more flexible empirical correction, a^{emp} , and a slightly different treatment of the polar contributions, Anderko and Pitzer (1993a,b) developed an EOS for the even more polar H₂O-NaCl binary system. This EOS includes a hard-sphere and a dipole representation of the associated NaCl molecules in the water mixture and was shown to provide very good predictions of volumetric and vapor–liquid equilibrium properties of NaCl-H₂O mixtures in the temperature range from 573 to 1200 K and up to 5 kbar (Anderko and Pitzer, 1993a). Duan et al. (1995, 2003) have further generalized this approach to include the gases, CO₂ and CH₄. This EOS predicts coexisting phase compositions and densities for the system NaCl-H₂O-CO₂-CH₄ with accuracy near that of experimental data when the CO₂ or CH₄ concentrations are not too large.

In the EOS description introduced here for the CaCl₂-H₂O and MgCl₂-H₂O systems, the H₂O molecules in the reference system are treated as hard spheres with dipole moments and the associated CaCl₂ and MgCl₂ solutes as hard spheres with quadrupole moments. Equations for the contributions to the Helmholtz free energy for dipole and quadrupole interactions in this reference system are available (Stell et al., 1972, 1974; Rushbrooke et al., 1973; Stephanopoulos et al., 1975; Twu et al., 1975; Gubbins and Twu, 1978; Twu and Gubbins, 1978). A very similar model for the CaCl₂-H₂O system has been reported by Jiang and Pitzer (JP model, 1995, 1996). However, there are important differences between the model presented here and the JP model. The JP model does not interpolate correctly from pure systems to mixtures. In addition, their formalism does not allow the inclusion of gases and other solute components such as NaCl. The EOS described here overcomes these problems and is consistent with the EOS published for the NaCl-KCl-H₂O and NaCl-H₂O-CO₂-CH₄ (Anderko and Pitzer, 1993a,b; Duan et al., 1995, 2003) systems.

2.1. The hard-sphere contribution

By comparison of EOS predictions with experimental phase equilibria data for non-polar systems, Dimitrelis and Prausnitz (1986) found that the hard-sphere mixture free energy equation developed by Boublik (1970) and Mansoori et al. (1971) provides a reference free energy with better mixing behavior than the one fluid model of Carnahan and Starling (1969). Therefore, in this work the hard-sphere contribution is taken to be,

$$\frac{a^{\text{hs}}}{RT} = \frac{\frac{3DE}{F}\eta_{\text{hs}} - \frac{E^3}{F^2}}{1 - \eta_{\text{hs}}} + \frac{\frac{E^3}{F^2}}{(1 - \eta_{\text{hs}})^2} + \left(\frac{E^3}{F^2} - 1\right) \ln(1 - \eta_{\text{hs}}), \quad (6)$$

where

$$D = \sum_{i=1}^n x_i \sigma_i, \quad (7)$$

$$E = \sum_{i=1}^n x_i \sigma_i^2, \quad (8)$$

and

$$F = \sum_{i=1}^n x_i \sigma_i^3. \quad (9)$$

σ_i is the hard-sphere size parameter for species i , determined by fitting PVT data for the pure system. An average co-volume, b , is defined as,

$$b = \frac{2}{3}\pi N_A F. \quad (10)$$

From which η_{hs} is defined by,

$$\eta_{\text{hs}} = b/4v. \quad (11)$$

It is also convenient to define a co-volume for species i for use in the a^{es} contributions as,

$$b_i = \frac{2}{3}N_A \pi \sigma_i^3. \quad (12)$$

In Eqs. (7)–(9), x_i is the mole fraction of species i in the mixture and N_A is Avogadro's number.

2.2. Electrostatic contribution

The electrostatic contributions to the free energy are computed from perturbation theory. The direct expansion converges slowly. However, Rushbrooke and Stell and coworkers (Stell et al., 1972, 1974; Rushbrooke et al., 1973) demonstrated that an accurate estimation of polar contributions could be obtained from the Padé approximation,

$$a^{\text{es}} = \frac{a_2}{1 - (a_3/a_2)}, \quad (13)$$

where a_2 and a_3 are the 2nd and 3rd terms in the perturbation series. a_3 contains two-body and three-body contributions,

$$a_3 = a_{3,2} + a_{3,3}. \quad (14)$$

Explicit expressions for a_2 , $a_{2,3}$, and $a_{3,3}$ have been given by Gubbins and Twu (Gubbins and Twu, 1978; Twu and Gubbins, 1978) as,

$$\begin{aligned} \frac{a_2}{RT} = & -\frac{3}{2\pi v} \left[\frac{2\pi}{9} \sum_i \sum_j x_i x_j \frac{b_i b_j}{b_{ij}} \tilde{\mu}_i^2 \tilde{\mu}_j^2 I_6^{\text{hs}}(v) \right. \\ & + \sum_i \sum_j x_i x_j \frac{b_i b_j^{5/3}}{2b_{ij}^{5/3}} \tilde{\mu}_i^2 \tilde{Q}_j^2 I_8^{\text{hs}}(v) \\ & \left. + \sum_i \sum_j x_i x_j \frac{7b_i^{5/3} b_j^{5/3}}{10b_{ij}^{7/3}} \tilde{Q}_i^2 \tilde{Q}_j^2 I_{10}^{\text{hs}}(v) \right], \end{aligned} \quad (15)$$

$$\frac{a_{3,2}}{RT} = \frac{54}{245\pi v} \sum_i \sum_j x_i x_j \frac{b_i^{5/2} b_j^{5/2}}{b_{ij}^4} \tilde{Q}_i^3 \tilde{Q}_j^3 I_{15}^{\text{hs}}(v), \quad (16)$$

and

$$\begin{aligned} \frac{a_{3,3}}{RT} = & \frac{9}{4\pi^2 v^2} \left[\frac{5\pi^2}{162} \sum_i \sum_j \sum_k x_i x_j x_k \frac{b_i b_j b_k}{(b_{ij} b_{ik} b_{jk})^{1/3}} \tilde{\mu}_i^2 \tilde{\mu}_j^2 \tilde{\mu}_k^2 I_{\text{ddd}}^{\text{hs}}(v) \right. \\ & + \frac{1}{480} \sum_i \sum_j \sum_k x_i x_j x_k \frac{b_i b_j b_k^{5/3}}{b_{ij}^{1/3} b_{ik}^{2/3} b_{jk}^{2/3}} \tilde{\mu}_i^2 \tilde{\mu}_j^2 \tilde{\mu}_k^2 I_{\text{ddq}}^{\text{hs}}(v) \\ & + \frac{1}{640} \sum_i \sum_j \sum_k x_i x_j x_k \frac{b_i b_j^{5/3} b_k^{5/3}}{b_{ij}^{2/3} b_{ik}^{2/3} b_{jk}^{2/3}} \tilde{\mu}_i^2 \tilde{Q}_j^2 \tilde{Q}_k^2 I_{\text{dq}}^{\text{hs}}(v) \\ & \left. + \frac{1}{6400} \sum_i \sum_j \sum_k x_i x_j x_k \frac{b_i^{5/3} b_j^{5/3} b_k^{5/3}}{b_{ij} b_{ik} b_{jk}} \tilde{Q}_i^2 \tilde{Q}_j^2 \tilde{Q}_k^2 I_{\text{qqq}}^{\text{hs}}(v) \right]. \end{aligned} \quad (17)$$

In the above equations, $I_m^{\text{hs}}(v)$ and $I_{\text{triplet}}^{\text{hs}}(v)$ are integrals of the hard-sphere distribution function. A convenient expansion in reciprocal molar volume for these integrals has been given by Larsen and coworkers (1977) in the form,

$$I_k^{\text{hs}}(v) = \sum_{i=0}^6 J_{i,k} \left[\frac{3b}{2\pi v} \right]^i \quad (k = 6, 8, 10, 15, \text{ddd}, \text{ddq}, \text{dqq}, \text{qqq}). \quad (18)$$

The extended virial series approximation coefficients, $J_{i,k}$, are listed in Table 1. ddd implies dipole–dipole–dipole contributions etc. The reduced dipole moment $\tilde{\mu}_i$ and reduced quadrupole moment \tilde{Q}_i are defined as,

$$\tilde{\mu}_i^2 = \frac{\mu_i^2}{kT\sigma_i^3}, \quad (19)$$

and

$$\tilde{Q}_i^2 = \frac{Q_i^2}{kT\sigma_i^5}. \quad (20)$$

where b_{ij} is given by,

$$b_{ij} = \left[(b_i^{1/3} + b_j^{1/3})/2 \right]^3. \quad (21)$$

2.3. The empirical correction

The empirical correction accounts for interactions (e.g. attractive dispersion forces), which are not well represented in the reference system. Anderko and Pitzer (1993a,b) developed the following expression for the empirical contribution to the compressibility, called perturbation term, based on their earlier work on truncated virial EOS (Anderko and Pitzer, 1991),

$$Z_{\text{per}} = -\frac{1}{RT} \left[\frac{a}{v} + \frac{acb}{2v^2} + \frac{3adb^2}{16v^3} + \frac{aeb^3}{16v^4} \right]. \quad (22)$$

In this equation, a , acb , adb^2 , and aeb^3 are related to the second, third, fourth, and fifth virial coefficients. These parameters together with b are evaluated from end-member (or pure system) system thermodynamic measurements. The parameters for mixed systems are calculated via the following mixing rules:

$$a = \sum_{i=1}^n \sum_{j=1}^n x_i x_j a_{ij}, \quad (23)$$

$$acb = \sum_{i=1}^n \sum_{j=1}^n \sum_{k=1}^n x_i x_j x_k (ac)_{ijk} b_{ijk}, \quad (24)$$

$$adb^2 = \sum_{i=1}^n \sum_{j=1}^n \sum_{k=1}^n \sum_{l=1}^n x_i x_j x_k x_l (ad)_{ijkl} b_{ijkl}^2, \quad (25)$$

and

$$aeb^3 = \sum_{i=1}^n \sum_{j=1}^n \sum_{k=1}^n \sum_{l=1}^n \sum_{m=1}^n x_i x_j x_k x_l x_m (ae)_{ijklm} b_{ijklm}^3, \quad (26)$$

where

$$b_{ijk} = \left[(b_i^{1/3} + b_j^{1/3} + b_k^{1/3})/3 \right]^3, \quad (27)$$

Table 1
Coefficients, $J_{i,k}$, in the extended virial series approximation in Eq. (18) taken from Larsen et al. (1977)

| k | $i=0$ | $i=1$ | $i=2$ | $i=3$ | $i=4$ | $i=5$ | $i=6$ |
|-----|----------|---------|----------|---------|---------|----------|---------|
| 6 | 1.0 | .84059 | −1.22057 | 1.44076 | 0.0 | 0 | 0 |
| 8 | 2.5133 | 2.7195 | 1.0423 | 0.2596 | 0.10970 | −0.573 | 0 |
| 10 | 1.7952 | 1.7551 | 1.0376 | 0.3890 | 0.15610 | −0.0082 | 0 |
| 15 | 1.0472 | 1.1631 | 0.8552 | 0.4506 | 0.1913 | 0.1465 | 0 |
| ddd | 1.000 | 1.02461 | −1.57017 | 1.64732 | 1.59943 | −1.77024 | 1.23196 |
| ddq | 139.491 | 241.935 | 163.958 | 57.0537 | 13.2686 | −22.3827 | 0 |
| dqq | 139.491 | 298.922 | 283.491 | 161.722 | 81.7788 | −35.8868 | 0 |
| qqq | 532.9586 | 1287.35 | 1447.98 | 1026.38 | 608.423 | −20.5065 | 0 |

$$b_{ijkl} = \left[(b_i^{1/3} + b_j^{1/3} + b_k^{1/3} + b_l^{1/3})/4 \right]^3, \quad (28)$$

$$b_{ijklm} = \left[(b_i^{1/3} + b_j^{1/3} + b_k^{1/3} + b_l^{1/3} + b_m^{1/3})/5 \right]^3, \quad (29)$$

$$a_{ij} = (a_i a_j)^{1/2} \alpha_{ij}, \quad (30)$$

$$(ac)_{ijk} = \left[(ac)_i (ac)_j (ac)_k \right]^{1/3} \gamma_{ijk}, \quad (31)$$

$$(ad)_{ijkl} = \left[(ad)_i (ad)_j (ad)_k (ad)_l \right]^{1/4} \delta_{ijkl}, \quad (32)$$

and

$$(ae)_{ijklm} = \left[(ae)_i (ae)_j (ae)_k (ae)_l (ae)_m \right]^{1/5} \varepsilon_{ijklm}. \quad (33)$$

α_{ij} , γ_{ijk} , δ_{ijkl} , and ε_{ijklm} are interaction parameters, which should be evaluated from mixed system data. The compressibility factor (Z) and partial fugacity coefficient ϕ_i can readily be obtained from Eqs. (2) and (3). Explicit expressions for the compressibility factor and fugacity coefficients for the hard-sphere and perturbation contributions were given by Duan et al. (1995). The equations for calculating electrostatic contributions including quadrupole interactions are given in Appendix A.

3. The experimental data

Pure system vapor pressure data for CaCl₂ and MgCl₂ have been reported by Chase et al. (1986) and liquid and supercooled liquid CaCl₂ density data by Janz et al. (1975). Thermodynamic properties of the mixed CaCl₂-H₂O and MgCl₂-H₂O systems have been measured for temperatures up to 973 K. All the available data in this temperature range are listed in Table 2. These include phase equilibrium data (vapor pressure, isopiestic measurements,

liquid-vapor equilibria, phase immiscibility, and coexisting phase compositions) and volumetric data (density and apparent volume).

Vapor pressures may be calculated from isopiestic data via the equation,

$$\ln P = \ln P^* - \frac{W}{1000} \left(\sum m_i \right) \varphi, \quad (34)$$

where P is the vapor pressure of the solution, P^* is the pure water vapor pressure at T . W is the molecular weight of water. m_i is the molality of solute species i , and φ is the measured osmotic coefficient. The sum is over all solute species. The vapor pressures calculated with the above equation from the isopiestic measurements of Holmes et al. (1994) may be compared to those reported by Wood et al. (1984) and Zarembo et al. (1980). The maximum deviation between these data sets is less than 0.4 bar or about 0.13 in terms of the osmotic coefficient for 523 and 573 K. However, for $T = 623$ K, the vapor pressures of Zarembo et al. (1980) are 2–4.5 bar lower than those reported by Wood et al. (1984). All these data are used for the parameterization.

Zhang and Frantz (1989) reported immiscibility data up to 973 K for concentrations of CaCl₂ up to 25 wt%. Shmulovich et al. (1995) and Bischoff et al. (1996) published phase equilibrium data from 653 to 873 K. Bischoff et al. (1996) observed that significant amount of HCl was produced from the hydrolysis of CaCl₂. We did not use these data for parameterization because the EOS reported here does not allow for hydrolysis. Apparent molar volume measurements for the CaCl₂ system have been reported by Gates and Wood (1989), Crovetto et al. (1993), and Oakes et al. (1995) cover the temperature range from 298 to 643 K. The deviations between these

Table 2
Thermodynamic data for the CaCl₂-H₂O and MgCl₂-H₂O systems at high TP

| System | Properties | T (K) | P (bar) | x | N | References |
|-------------------------------------|---------------------------|---------|-----------|-------------|-----|------------------------------|
| CaCl ₂ -H ₂ O | P (sat) | 423–623 | 5–165 | 0–0.1 | 40 | Zarembo et al. (1980) |
| | P (sat) | 473–623 | 15–160 | 0.01–0.11 | 107 | Wood et al. (1984) |
| | P (sat) | 523–673 | 5–230 | 0.08–sat | 33 | Ketsko et al. (1984) |
| | Immiscibility | 873–973 | 1000–1900 | 0.0–0.04 | 20 | Zhang and Frantz (1989) |
| | VLE | 653–773 | 230–800 | 0.0–0.1 | 90 | Bischoff et al. (1996) |
| | φ | 444–524 | 5–40 | 0–0.08 | 124 | Holmes et al. (1994) |
| | v_φ | 298–523 | 70–415 | 0.242–6.15 | 55 | Oakes et al. (1995) |
| | v_φ | 323–597 | 1–207 | 0–0.1 | 96 | Gates and Wood (1989) |
| | v_φ and P (sat) | 623–643 | 167–221 | 0.004–0.055 | 82 | Crovetto et al. (1993) |
| | VLE | 673–873 | 271–1324 | 0–0.12 | 50 | Shmulovich et al. (1995) |
| | K_1 and K_2 | 298–873 | 0–250 | 0.001–0.005 | 200 | Frantz and Marshall (1982) |
| MgCl ₂ -H ₂ O | P (sat) | 573–623 | 10–163 | 0–0.3 | 38 | Urusova and Valyashko (1983) |
| | P (sat) | 523 | 3–38 | 0–0.49 | 10 | Urusova and Valyashko (1984) |
| | Density | 298–573 | 20–300 | 0.008–0.032 | 81 | Pepinov et al. (1992) |
| | v_φ | 298–627 | 100–300 | 0.0005–0.05 | 143 | Obsil et al. (1997) |
| | VLE | 673–973 | 285–1048 | 0–0.12 | 42 | Shmulovich et al. (1995) |
| | K_1 and K_2 | 298–873 | 0–250 | 0.001–0.005 | 134 | Frantz and Marshall (1982) |

N —number of measurements; P (sat)—saturation pressure; φ —osmotic pressure; v_φ —apparent molar volume; K_1 — $a_{\text{CaCl}^+} a_{\text{Cl}^-} / a_{\text{CaCl}_2}$, K_2 — $a_{\text{Ca}^{++}} a_{\text{Cl}^-} / a_{\text{CaCl}^+}$, x —mole fraction.

data sets are less than 0.5% in molar volume in overlapping TPX ranges.

The data for the $\text{MgCl}_2\text{-H}_2\text{O}$ system (Table 2) are for different T - P ranges, except for the density data by Pepinov et al. (1992) and Obsil et al. (1997) with some overlap in the TP space. The molar volumes reported by Pepinov et al. (1992) are about 1% higher than those by Obsil et al. (1997). Other data for the $\text{MgCl}_2\text{-H}_2\text{O}$ system up to 627 K have been summarized by Wang et al. (1998b).

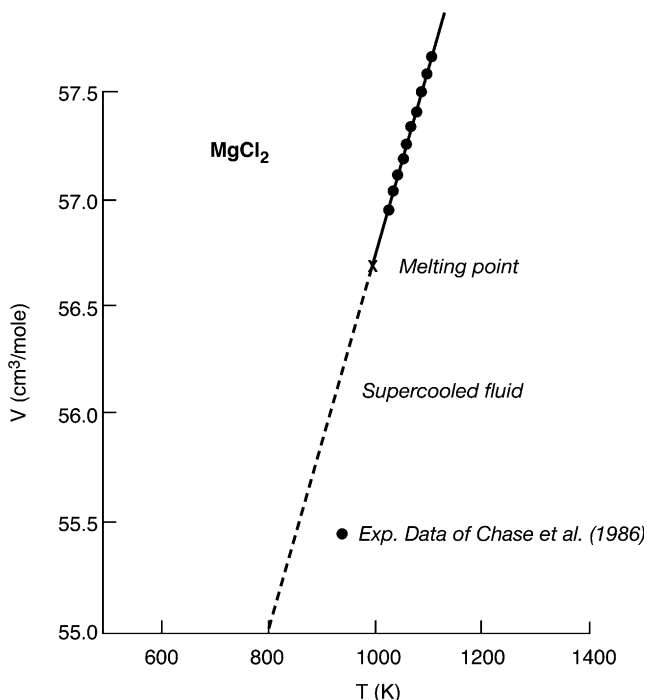


Fig. 1. Molar volumes of pure liquid MgCl_2 calculated from this EOS (solid line) vs. the experimental data of Chase et al. (1986). Dashed line represents molar volume of supercooled liquid.

4. Evaluation of the EOS parameters

4.1. Pure system parameters

The EOS parameters for pure components include the co-volume b_i , the dipole moment μ_i of water, the quadrupole moments Q_i of CaCl_2 and MgCl_2 , and the empirical contribution parameters a_i , c_i , d_i , and e_i . The parameters for pure H_2O were slightly modified from Anderko and Pitzer (1993a) to give better predictions of vapor pressures especially in the high temperature range. Our implementation of the Jiang and Pitzer (1996) EOS for the $\text{CaCl}_2\text{-H}_2\text{O}$ system reproduced the pure CaCl_2 melt properties, but did not yield correct properties in the binary. We retained the Jiang and Pitzer quadrupole moment and co-volume and reevaluated the perturbation parameters (a_i , c_i , d_i , and e_i). Our parameterization for pure CaCl_2 accurately reproduces the vapor pressure (Chase et al., 1986) and the density data of the liquid and the supercooled liquid (Janz et al., 1975).

The quadrupole moment for MgCl_2 was evaluated using the method introduced by Rittner (1951) and used by Jiang and Pitzer (1996) to estimate Q for CaCl_2 . For MgCl_2 molecule, the minimum distance between nuclei of Mg and Cl, r_e , was taken to be 2.18 (Chase et al., 1986) and the reduced moment was taken from Rittner (1951). Given these values the quadrupole moment for MgCl_2 is 8.344×10^{-26} esu. The parameters a , b , c , d , and e were evaluated from the density data of Janz et al. (1975). The molar volume of the MgCl_2 melt as a function of T is well predicted, as shown in Fig. 1. The parameters for the pure components are given in Table 3.

4.2. The $\text{CaCl}_2\text{-H}_2\text{O}$ system

The EOS for the binary systems were formed using the end-member EOS mixing rules, Eqs. (23)–(33), which contain parameters, α_{ij} , γ_{ijk} , δ_{ijkl} , and ε_{ijklm} . For the $\text{CaCl}_2\text{-H}_2\text{O}$ system, the parameters were evaluated from the vapor pressure, phase equilibrium and volumetric data included in Table 2. The immiscibility data of Zhang and Frantz (1989)

Table 3
The parameters of the EOS for pure components

| Parameter (U) | H_2O | CaCl_2 | MgCl_2 |
|--------------------------------------|--|---|--|
| M (D) | 1.85 | 0.0 | 0.0 |
| Q (esu) | 0.0 | $-2.284\text{E}-25$ | $-8.344\text{E}-26$ |
| a ($\text{bar cm}^6/\text{mol}$) | $(1.718248 + 1.828379/T_r)$ $+1.546648/T_r^2$ $+0.1022/T_r^4) \times 10^6$ | $(4.71862036$ $+6.42756576\text{E}-03T$ $-1.27513\text{E}-06T^2) \times 10^7$ | $(4.12268352$ $+7.24471\text{E}-03T$ $-1.69515\text{E}-06T^2) \times 10^7$ |
| b (cm^3) | 28.4959 | $138.81 - 0.005109T + 1.732\text{E}-6T^2$ | $143.38 - 0.02051818T + 7.727272T^2$ |
| c | $2.953548 - 8.874823/T_r$ $+3.179334/T_r^2$ $-0.168698/T_r^4$ | -1 | -1 |
| d | $2.139339 + 9.442203/T_r$ $-3.144017/T_r^2$ $+0.149539/T_r^4$ | 2 | 2 |
| e | -9 | -1 | -1 |

$$T_r = T/647.067.$$

was treated as vapor pressure data with equal weight. Because the prediction of phase equilibrium is more sensitive to the EOS parameters, we gave more weight to vapor pressure and phase equilibrium data than to volumetric data. The vapor pressure data of Zarembo et al. (1980), Wood et al. (1984), and Ketsko et al. (1984) from 523 to 673 K are reproduced with accuracy close to that of the experiments using this EOS as shown in Figs. 2 and 3. The immiscibility boundary data at 873 and 973 K of Zhang and Frantz (1989) are also well predicted, as shown in Fig. 4.

Vapor-liquid coexistence phase composition data have been reported by Shmulovich et al. (1995) and Bischoff et al. (1996) from 653 to 873 K for conditions close to the mixture critical pressures. Bischoff et al. (1996) noted significant HCl production especially in the low-pressure region presumably from hydrolysis. The more volatile HCl segregates in the vapor phase causing a high concentration of HCl (relative to $CaCl_2$). Hydrolysis is not considered in this model, and these data are not used in the parameterization. This EOS does not predict correct vapor phase compositions under these temperature-pressure conditions. The predicted liquid phase compositions agree well with the data as shown in Fig. 5.

Apparent molar volume measurements for the $CaCl_2$ - H_2O system have been reported by Gates and Wood (1989), Crovetto et al. (1993), and Oakes et al. (1995) for temperatures up to 643 K and pressures up to 400 bar. The deviations between the different data sets are less than 0.5%. These data are accurately predicted by the EOS as shown in Figs. 6–8. Adding a small amount of $CaCl_2$ to water significantly decreases the molar volume of the solution, especially at higher temperatures. This behavior is well described by the model.

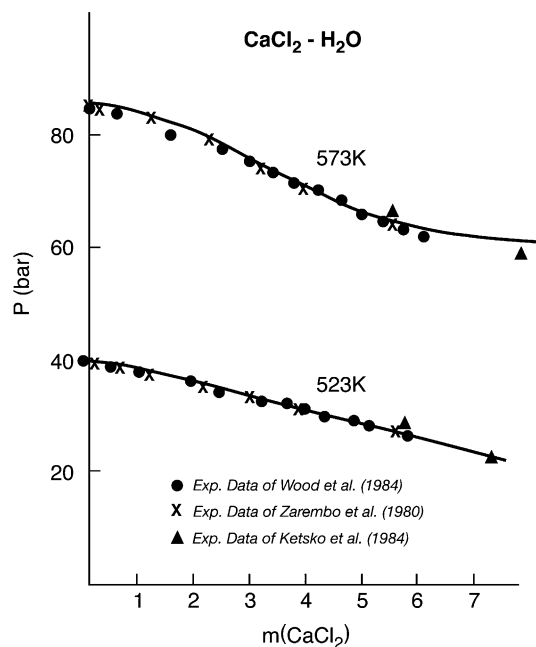


Fig. 2. Water vapor pressure calculated from this EOS (solid line) vs. experimental data for the $CaCl_2$ - H_2O system at 523 and 573 K.

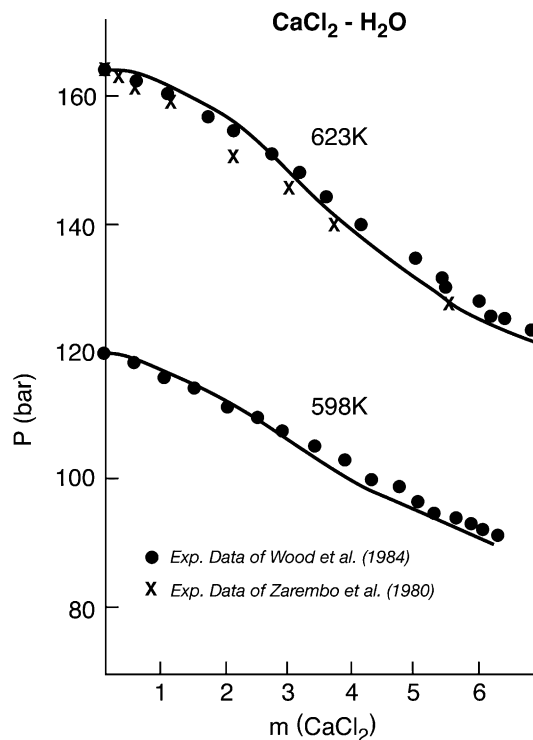


Fig. 3. Water vapor pressure calculated from this EOS (solid line) vs. experimental data for the $CaCl_2$ - H_2O system at 598 and 623 K.

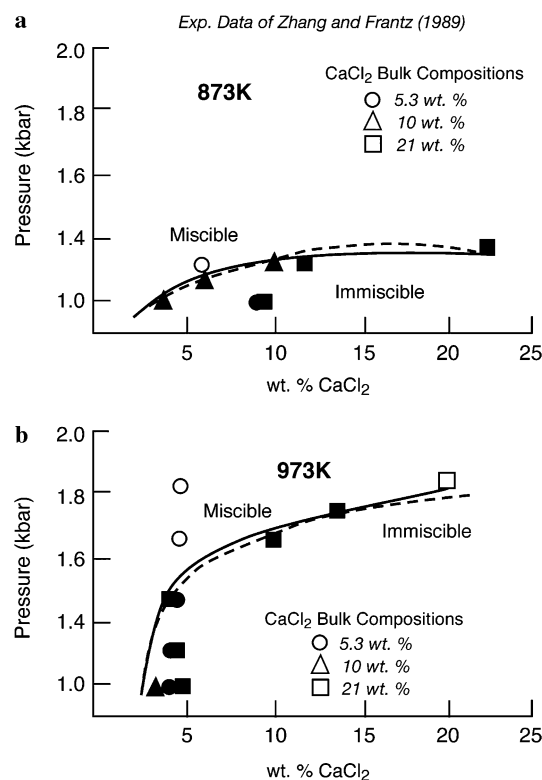


Fig. 4. Measured immiscibility boundaries (dashed lines) in the $CaCl_2$ - H_2O system (Zhang and Frantz, 1989) compared to the predictions of this EOS (solid lines).

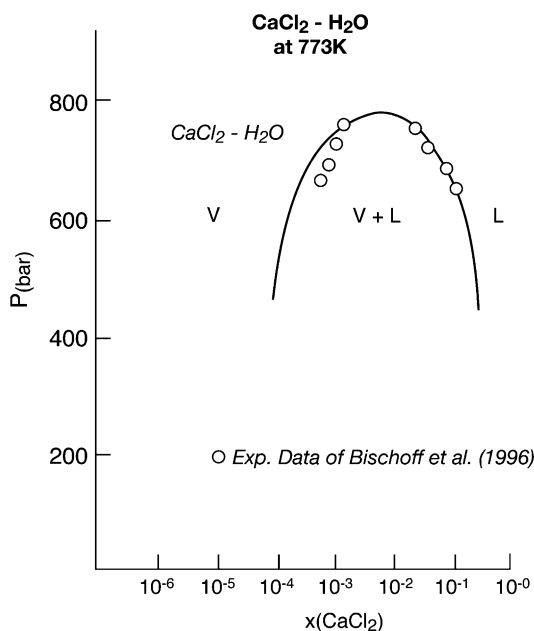


Fig. 5. Liquid–vapor phase compositions in the system $\text{CaCl}_2\text{-H}_2\text{O}$ calculated from this EOS (solid line) vs. experimental measurements.

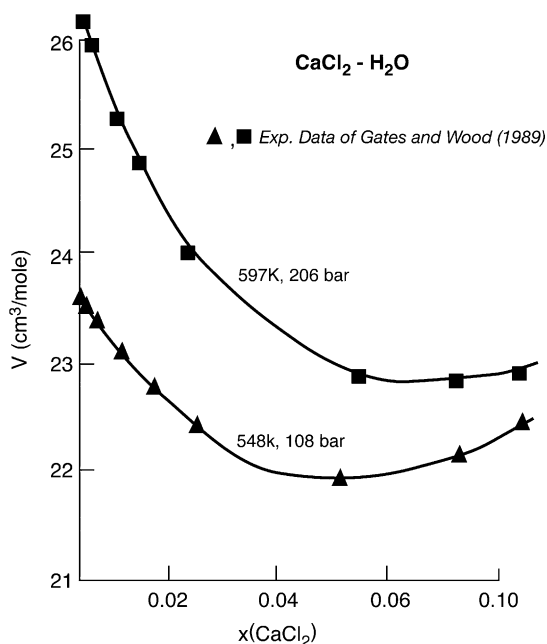


Fig. 6. Calculated molar volumes of aqueous CaCl_2 solutions (solid lines) vs. experimental measurements.

4.3. The $\text{MgCl}_2\text{-H}_2\text{O}$ system

The mixing parameters reported in Table 4 for the $\text{MgCl}_2\text{-H}_2\text{O}$ binary were evaluated from the liquid–vapor equilibrium, vapor pressure and volumetric data listed in Table 2. The vapor pressure data for this system cover a range from below 523 to 623 K and are accurately predicted by this EOS as shown in Fig. 9. The compositions of coexisting phases for this binary (Shmulovich et al., 1995)

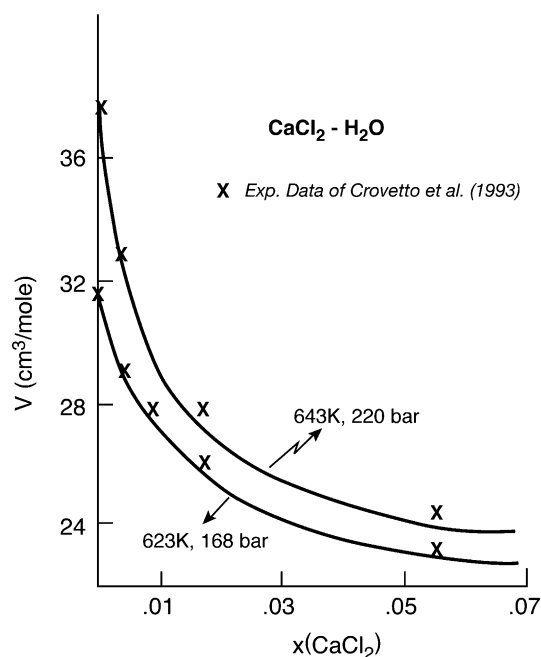


Fig. 7. Calculated molar volumes of aqueous CaCl_2 solutions (solid lines) vs. experimental measurements.

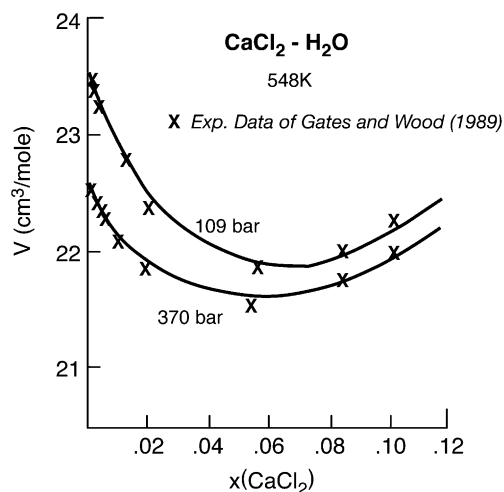


Fig. 8. Calculated molar volumes of aqueous CaCl_2 solutions (solid lines) vs. experimental measurements.

are predicted with reasonable accuracy, Fig. 10. The vapor compositions are more accurately predicted for the $\text{MgCl}_2\text{-H}_2\text{O}$ system, in which hydrolysis has not been observed, than for the $\text{CaCl}_2\text{-H}_2\text{O}$ system. The accuracy of the EOS decreases as the pressure approaches the critical value for the mixture. As in the $\text{CaCl}_2\text{-H}_2\text{O}$ system, the volumetric data for this system are accurately represented by the EOS, Figs. 11 and 12.

5. Discussion

In this article, an equation of state capable of describing the thermodynamics of the systems $\text{MgCl}_2\text{-H}_2\text{O}$ and

Table 4
Mixing parameters

| Parameters | H_2O - $CaCl_2$ | H_2O - $MgCl_2$ |
|-------------------|--|--|
| α | 0.9 | 1 |
| γ_{ij} | $0.911715 + 1.8662E-04T - 3.619845T^2$ | $1.5462 - 1.35516E-03T + 5.5942E-07T^2$ ($T < 592$ K) $-1.8947 + 8.035E-03 - 5.484E-06T^2$ ($T \geq 592$ K) |
| γ_{ijj} | $1.1553 + 2.16406E-4T$ | $1.1854 + 0.0002T$ |
| δ_{ijj} | 1.05 | 1.04 |
| δ_{iij} | 1.0 | 1.0 |
| δ_{jjj} | 1.0 | 0.97 |
| ϵ_{ijj} | 1.24 | 1 |
| ϵ_{iij} | 1.24 | 1 |
| ϵ_{jjj} | 1.24 | 1 |
| ϵ_{ijij} | 1.24 | 1 |

i — H_2O ; j — $CaCl_2$ or $MgCl_2$. All other parameters not listed here, such as γ_{iii} , are set as 1.

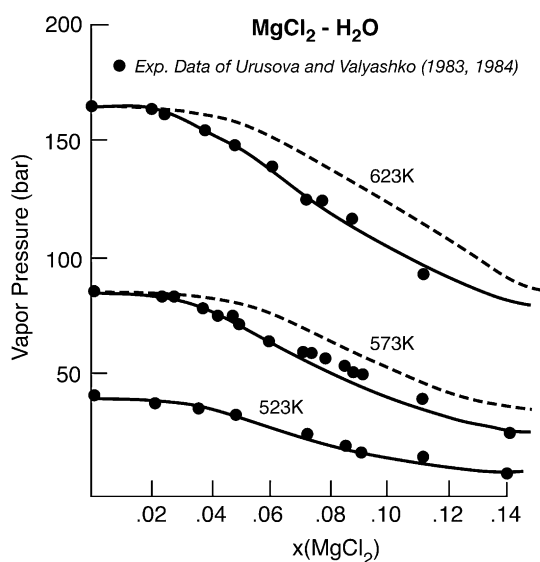


Fig. 9. Calculated Water vapor pressures (solid line) vs. experimental data for the $MgCl_2$ - H_2O system. The dashed lines are the vapor pressures calculated from the model of Wang et al. (1998b).

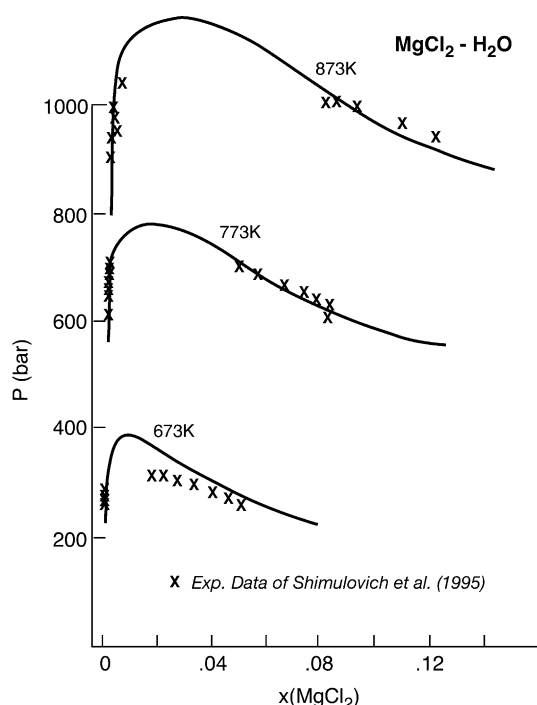


Fig. 10. Calculated Liquid-vapor phase compositions of aqueous $MgCl_2$ solutions (solid line) vs. experimental measurements.

$CaCl_2$ - H_2O are reported. Following Anderko and Pitzer (1993a,b), Jiang and Pitzer (1995, 1996), and Duan et al. (1995, 2003), the EOS is based on the separation of the Helmholtz free energy into a reference system and an empirical correction term. The solute species, $CaCl_2$ and $MgCl_2$, are assumed to be associated for the temperature range ($T > 523$ K) (Gunter and Eugster, 1978; Frantz and Marshall, 1982). The reference system is idealized as a mixture of hard-sphere dipoles (water molecules) and hard-sphere quadrupoles (for the $CaCl_2$ and $MgCl_2$ solute molecules). An empirical correction is necessary to correct for deficiencies in this reference state and to account for attractive dispersion forces. The inclusion of the polar behavior at the molecular level improves the interpolation and extrapolation of the EOS and decreases the role of the empirical correction. These EOS accurately describe the phase behavior and the volumetric properties for the $CaCl_2$ - H_2O and $MgCl_2$ - H_2O systems in the temperature

range from 523 to 973 K for pressures up to about 1500 bar as shown in Figs. 2–11. It is possible that these models can be extrapolated to higher temperatures and pressures because the end-member EOS provide accurate predictions for higher temperature and pressures and the mixing rules are only slightly dependent on temperature and independent of pressure. The formalism presented in Eqs. (6)–(33) allows the generalization of this EOS to systems containing alkali halide and gases. In fact, this formalism will reduce to the EOS of the $NaCl$ - H_2O system reported by Anderko and Pitzer (1993a,b), and to the EOS of the H_2O - CO_2 - $NaCl$ system of Duan et al. (1995), though the applicable temperature will be above 573 K.

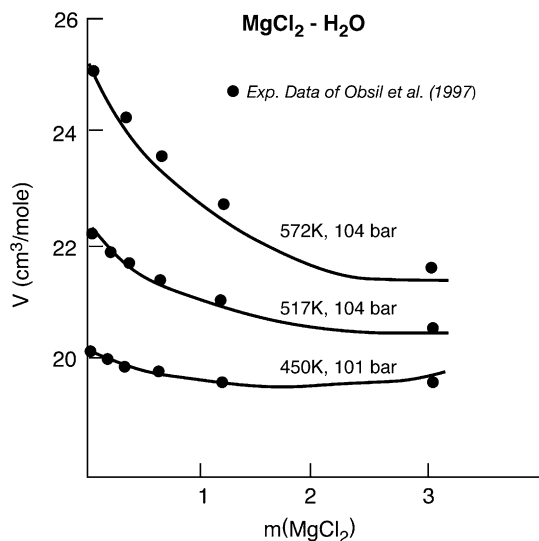


Fig. 11. Calculated molar volumes of aqueous MgCl_2 solutions (solid lines) vs. experimental measurements.

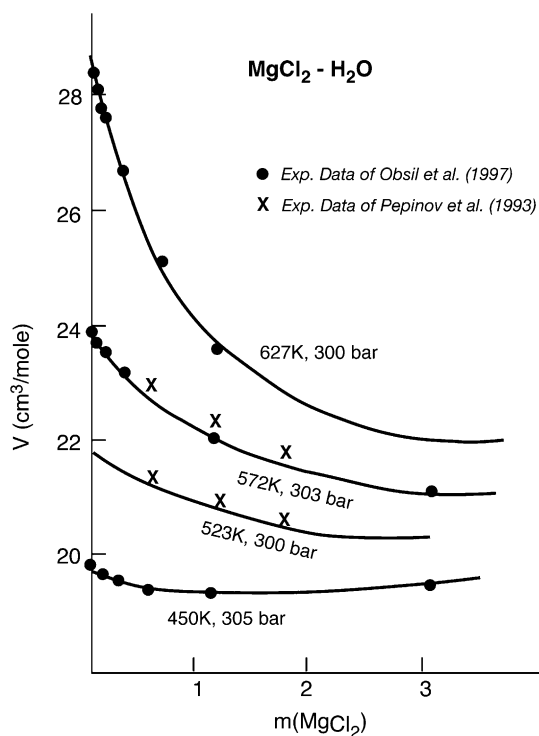


Fig. 12. Calculated molar volumes of aqueous MgCl_2 solutions (solid lines) vs. experimental measurements.

In Fig. 9 the calculated vapor pressure from this EOS and the EOS of Wang et al. (1998a,b) are compared with experimental data. For $T = 573$ and 623 K, the model of Wang et al. (1998b), which is based on the complete dissociation model of Pitzer (1973), fails to provide the correct behavior, suggesting that the associated nature of the solute molecules as used in this EOS is important in this high temperature region.

Table 5
Predicted saturation pressures in MgCl_2 - CaCl_2 - H_2O mixtures

| T (K) | $x_{\text{H}_2\text{O}}$ | x_{CaCl_2} | x_{MgCl_2} | P (saturation, bar) |
|---------|--------------------------|---------------------|---------------------|-----------------------|
| 623 | 0.9 | 0.1 | 0.0 | 125.1 |
| 623 | 0.9 | 0.0 | 0.1 | 108.0 |
| 623 | 0.9 | 0.05 | 0.05 | 145.9 |

Eqs. (5)–(33) provide a formalism for combining these two binary models to form an EOS for the ternary MgCl_2 - CaCl_2 - H_2O system. Anderko and Pitzer successfully used this approach for the NaCl - KCl - H_2O system (Anderko and Pitzer, 1993b) and Duan et al. (2003) developed a model for the quaternary NaCl - H_2O - CH_4 - CO_2 system. Since there is very little data in the ternary or quaternary systems, these EOS relied solely on parameters from the binary systems to predict the higher order system behavior. The calculation of mixed system parameters using this approach is straight forward. However, when used for the CaCl_2 - MgCl_2 - H_2O system, very non-ideal mixing behavior is obtained. We view the prediction as somewhat suspect. For example, predicted saturation pressures for various mixed solutions are presented in Table 5 for a 90% H_2O + 5% CaCl_2 + 5% MgCl_2 mixture. If we lump all the salt into the CaCl_2 component, we obtain a saturation pressure of 125.1 bar. If we chose MgCl_2 to be the salt component, we obtain 108 bar. We would expect the mixed salt system to have a saturation pressure somewhere between these two extremes. However, the result of our model is considerably larger, 145 bar. This could be due very non-ideal behavior in this system or to our assumption of mixing based solely on the binary parameters. Unfortunately, with no ternary data available, there is no way to evaluate the accuracy of this mixing approach. We hope that in the future data will be taken for ternary mixed systems which can be used to guide the development of mixture models.

Acknowledgments

The support of the following grants is acknowledged: NSF EAR-0126331, DOE DE-FG02-02ER15311, DOE-FG36-99ID13745 and ACS-PRF37196AC9, and by Zhenhao Duan's Key Project Funds (#40537032) and Outstanding Young Scientist Funds (#40225008) awarded by the National Science Foundation of China. Thank the three anonymous reviewers and Dr. E. Oelkers for their constructive suggestions.

Associate editor: Eric H. Oelkers

Appendix A. Compressibility factor and fugacity coefficient

A.1. Compressibility factor

The compressibility factor can be found from Eq. (2), where

$$Z = Z_{\text{hd}} + Z_{\text{es}} + Z_{\text{per}}. \quad (\text{A.1})$$

Z_{hd} and Z_{per} are given by Eqs. (5) and (24) of Duan et al. (1995). Z_{es} may be derived from Eq. (2),

$$Z_{\text{es}} = v \frac{\left(1 - \frac{2a_3}{a_2}\right) \frac{\partial(a_2/RT)}{\partial v} + \frac{\partial(a_{3,2}/RT)}{\partial v} + \frac{\partial(a_{3,3}/RT)}{\partial v}}{(1 - A_3/A_2)^2}, \quad (\text{A.2})$$

where

$$\begin{aligned} \frac{\partial(a_2/RT)}{\partial v} = & \frac{3}{2\pi v^2} \left[\frac{2\pi}{9} \sum_i \sum_j x_i x_j \frac{b_i b_j}{b_{ij}} \tilde{\mu}_i^2 \tilde{\mu}_j^2 \left(I_6^{\text{hs}} - v \frac{\partial I_6^{\text{hs}}}{\partial v} \right) \right. \\ & + \sum_i \sum_j x_i x_j \frac{b_i b_j^{5/3}}{2b_{ij}^{5/3}} \tilde{\mu}_i^2 \tilde{\mu}_j^2 I_8^{\text{hs}} \left(I_8^{\text{hs}} - v \frac{\partial I_8^{\text{hs}}}{\partial v} \right) \\ & \left. + \sum_i \sum_j x_i x_j \frac{7b_i^{5/3} b_j^{5/3}}{10b_{ij}^{7/3}} \tilde{Q}_i^2 \tilde{Q}_j^2 I_{10}^{\text{hs}} \left(I_{10}^{\text{hs}} - v \frac{\partial I_{10}^{\text{hs}}}{\partial v} \right) \right], \quad (\text{A.3}) \end{aligned}$$

$$\begin{aligned} \frac{\partial(a_{3,2}/RT)}{\partial v} = & \frac{54}{245\pi v^2} \sum_i \sum_j x_i x_j \\ & \times \frac{b_i^{5/2} b_j^{5/2}}{b_{ij}^4} \tilde{Q}_i^3 \tilde{Q}_j^3 I_{15}^{\text{hs}}(v^*) \left(I_{15}^{\text{hs}} - v \frac{\partial I_{15}^{\text{hs}}}{\partial v} \right), \quad (\text{A.4}) \end{aligned}$$

and

$$\begin{aligned} \frac{\partial(a_{3,3}/RT)}{\partial v} = & \frac{9}{4\pi^2 v^2} \left[\frac{5\pi^2}{162} \sum_i \sum_j \sum_k x_i x_j x_k \right. \\ & \times \frac{b_i b_j b_k}{(b_{ij} b_{ik} b_{jk})^{1/3}} \tilde{\mu}_i^2 \tilde{\mu}_j^2 \tilde{\mu}_k^2 \left(I_{\text{ddd}}^{\text{hs}} - v \frac{\partial I_{\text{ddd}}^{\text{hs}}}{\partial v} \right) \\ & + \frac{1}{480} \sum_i \sum_j \sum_k x_i x_j x_k \frac{b_i b_j b_k^{5/3}}{b_{ij}^{1/3} b_{ik}^{2/3} b_{jk}^{2/3}} \tilde{\mu}_i^2 \tilde{\mu}_j^2 \tilde{Q}_k^2 \\ & \times \left(I_{\text{ddq}}^{\text{hs}} - v \frac{\partial I_{\text{ddq}}^{\text{hs}}}{\partial v} \right) + \frac{1}{640} \sum_i \sum_j \sum_k x_i x_j x_k \\ & \times \frac{b_i b_j^{5/3} b_k^{5/3}}{b_{ij}^{2/3} b_{ik}^{2/3} b_{jk}^{2/3}} \tilde{\mu}_i^2 \tilde{\mu}_j^2 \tilde{Q}_k^2 \left(I_{\text{dqq}}^{\text{hs}} - v \frac{\partial I_{\text{dqq}}^{\text{hs}}}{\partial v} \right) \\ & + \frac{1}{6400} \sum_i \sum_j \sum_k x_i x_j x_k \frac{b_i^{5/3} b_j^{5/3} b_k^{5/3}}{b_{ij} b_{ik} b_{jk}} \tilde{Q}_i^2 \tilde{Q}_j^2 \tilde{Q}_k^2 \\ & \left. \times \left(I_{\text{qqq}}^{\text{hs}} - v \frac{\partial I_{\text{qqq}}^{\text{hs}}}{\partial v} \right) \right]. \quad (\text{A.5}) \end{aligned}$$

In the above equations,

$$\begin{aligned} \frac{\partial I_K^{\text{hs}}}{\partial v} = & \sum_{i=0}^6 J_{i,k} \left(\frac{3b}{2\pi} \right)^i \left(\frac{-i}{v^{i+1}} \right) \\ (k = & 6, 8, 10, 15, \text{ddd}, \text{ddq}, \text{dq}, \text{qqq}), \quad (\text{A.6}) \end{aligned}$$

where b is the co-volume and the $J_{i,k}$ are the extended virial series approximation coefficients, listed in Table 1 (Larsen et al., 1977). ddd implies the dipole–dipole–dipole contribution, etc.

A.2. Fugacity coefficient

The fugacity coefficient ϕ_i may be found from Eq. (3),

$$\ln \phi_i = \left[\frac{\partial(a^{\text{res}}/RT)}{\partial n_i} \right]_{v,T,n_{j \neq i}} - \ln Z + Z - 1 \quad (\text{A.7})$$

($\mu_i - \mu_i^{\text{id}}$) is given by the sum of the hard-sphere, electrostatic and perturbation contributions,

$$\left[\frac{\partial(a^{\text{res}}/RT)}{\partial n_i} \right]_{v,T,n_{j \neq i}} = \frac{\Delta\mu_{i,\text{hd}}}{RT} + \frac{\Delta\mu_{i,\text{es}}}{RT} + \frac{\Delta\mu_{i,\text{per}}}{RT}, \quad (\text{A.8})$$

where $\Delta\mu_{i,\text{hd}}/RT$ and $\Delta\mu_{i,\text{per}}/RT$ are given in the Appendix of Duan et al. (2003). However, there was an error in the expression of $\Delta\mu_{i,\text{hd}}/RT$, which should be

$$\frac{\Delta\mu_{i,\text{hd}}}{RT} = \left[\frac{\partial(a/RT)}{\partial n_i} \right]_{v,T,n_{j \neq i}} \quad (\text{A.9})$$

$\Delta\mu_{i,\text{es}}/RT$, which includes the dipole–dipole, dipole–quadrupole, and quadrupole–quadrupole interactions, is given by,

$$\begin{aligned} \frac{\Delta\mu_{i,\text{es}}}{RT} = & \left[\frac{\partial(na_{\text{es}}/RT)}{\partial n_i} \right]_{v,T,n_{j \neq i}} \\ = & \frac{\left(1 - \frac{2a_3}{a_2}\right) \frac{\partial(na_2)}{\partial n_i} + \frac{\partial(na_{3,2})}{\partial n_i} + \frac{\partial(na_{3,3})}{\partial n_i}}{\left(1 - \frac{a_3}{a_2}\right)^2}, \quad (\text{A.10}) \end{aligned}$$

where

$$\begin{aligned} \frac{\partial(na_2/RT)}{\partial n_i} = & -\frac{3}{2\pi v} \left[\frac{4\pi}{9} \sum_j x_j \frac{b_i b_j}{b_{ij}} \tilde{\mu}_i^2 \tilde{\mu}_j^2 I_6^{\text{hs}} \right. \\ & + \frac{2\pi}{9} \sum_i \sum_j x_i x_j \frac{b_i b_j}{b_{ij}} \tilde{\mu}_i^2 \tilde{\mu}_j^2 \left(n \frac{\partial I_6^{\text{hs}}}{\partial n_i} \right) \\ & + \sum_{j \neq i} x_j \frac{b_i b_j^{5/3}}{b_{ij}^{5/3}} \tilde{\mu}_i^2 \tilde{Q}_j^2 I_8^{\text{hs}} + \sum_{j \neq i} x_j \frac{b_i^{5/3}}{b_{ij}^{5/3}} \tilde{\mu}_i^2 \tilde{Q}_j^2 I_8^{\text{hs}} \\ & + \sum_i \sum_j x_i x_j \frac{b_i b_j}{b_{ij}} \tilde{\mu}_i^2 \tilde{\mu}_j^2 \left(n \frac{\partial I_8^{\text{hs}}}{\partial n_i} \right) \\ & + \frac{7}{5} \sum_j x_j \frac{b_i^{5/3} b_j^{5/3}}{b_{ij}^{7/3}} \tilde{Q}_i^2 \tilde{Q}_j^2 I_{10}^{\text{hs}} \\ & \left. + \frac{7}{10} \sum_j x_i x_j \cdot \frac{(b_i b_j)^{5/3}}{b_{ij}} \tilde{Q}_i^2 \tilde{Q}_j^2 \left(n \frac{\partial I_{10}^{\text{hs}}}{\partial n_i} \right) \right], \quad (\text{A.11}) \end{aligned}$$

$$\begin{aligned} \frac{\partial(na_{3,2}/RT)}{\partial n_i} = & \frac{54}{245\pi v} \left[2 \sum_j x_j \tilde{Q}_i^3 \tilde{Q}_j^3 \frac{b_i^{5/2} b_j^{5/2}}{b_{ij}^4} I_{15}^{\text{hs}} \right. \\ & \left. + \sum_i \sum_j x_i x_j \tilde{Q}_i^3 \tilde{Q}_j^3 \frac{b_i^{5/2} b_j^{5/2}}{b_{ij}^4} \left(n \frac{\partial I_{15}^{\text{hs}}}{\partial n_i} \right) \right] \quad (\text{A.12}) \end{aligned}$$

and

$$\begin{aligned}
& \frac{\partial(na_{3,3}/RT)}{\partial n_i} \\
&= \frac{9}{4\pi^2 v^2} \left[\frac{15\pi^2}{162} \sum_j \sum_k x_j x_k \tilde{\mu}_i^2 \tilde{\mu}_j^2 \tilde{\mu}_k^2 \frac{b_i b_j b_k}{(b_{ij} b_{ik} b_{jk})^{1/3}} I_{ddd}^{hs} \right. \\
&+ \sum_i \sum_j \sum_k \frac{5\pi^2}{162} x_i x_j x_k \tilde{\mu}_i^2 \tilde{\mu}_j^2 \tilde{\mu}_k^2 \frac{b_i b_j b_k}{(b_{ij} b_{ik} b_{jk})^{1/3}} \\
&\times \left(n \frac{\partial I_{ddd}^{hs}}{\partial n_i} \right) + \frac{1}{240} \sum_j \sum_{k \neq i} x_j x_k \tilde{\mu}_i^2 \tilde{\mu}_j^2 \tilde{Q}_k^2 \\
&\times \frac{b_i b_j b_k^{5/3}}{b_{ij}^{1/3} (b_{ik} b_{jk})^{2/3}} I_{ddq}^{hs} + \frac{1}{480} \sum_{j \neq i} \sum_{k \neq i} x_j x_k \tilde{Q}_i^2 \tilde{\mu}_j^2 \tilde{\mu}_k^2 \\
&\times \frac{b_i^{5/3} b_j b_k}{b_{ij}^{1/3} (b_{ik} b_{jk})^{2/3}} I_{ddq}^{hs} \\
&+ \frac{1}{480} \sum_i \sum_j \sum_k x_i x_j x_k \tilde{\mu}_i^2 \tilde{\mu}_j^2 \tilde{Q}_k^2 \\
&\times \frac{b_i b_j b_k^{5/3}}{(b_{ij})^{1/3} (b_{ik} b_{jk})^{2/3}} \left(n \frac{\partial I_{ddq}^{hs}}{\partial n_i} \right) \\
&+ \frac{1}{640} \sum_j \sum_{k \neq i} x_j x_k \tilde{\mu}_i^2 \tilde{Q}_j^2 \tilde{Q}_k^2 \frac{b_i (b_j b_k)^{5/3}}{(b_{ij} b_{ik})^{2/3} b_{jk}} I_{dqq}^{hs} \\
&+ \frac{1}{320} \sum_{j \neq i} \sum_{k \neq i} x_j x_k \tilde{Q}_i^2 \tilde{\mu}_j^2 \tilde{Q}_k^2 \frac{b_i (b_j b_k)^{5/3}}{(b_{ij} b_{ik})^{2/3} b_{jk}} I_{dqq}^{hs} \\
&+ \frac{1}{640} \sum_i \sum_j \sum_k x_i x_j x_k \tilde{\mu}_i^2 \tilde{Q}_j^2 \tilde{Q}_k^2 \frac{b_i (b_j b_k)^{5/3}}{(b_{ij} b_{ik})^{5/3} b_{jk}} \\
&\times \left(n \frac{\partial I_{dqq}^{hs}}{\partial n_i} \right) + \frac{3}{6400} \sum_i \sum_j \sum_k x_j x_k \tilde{Q}_i^2 \tilde{Q}_j^2 \tilde{Q}_k^2 \\
&\times \frac{(b_i b_j b_k)^{5/3}}{b_{ij} b_{ik} b_{jk}} I_{qqq}^{hs} + \frac{1}{6400} \sum_i \sum_j \sum_k \\
&\times x_i x_j x_k \tilde{Q}_i^2 \tilde{Q}_j^2 \tilde{Q}_k^2 \frac{(b_i b_j b_k)^{5/3}}{b_{ij} b_{ik} b_{jk}} \left(n \frac{\partial I_{qqq}^{hs}}{\partial n_i} \right) \left. \right]. \quad (A.13)
\end{aligned}$$

In these equations $\frac{\partial I_{ijk}^{hs}}{\partial n_i}$ is given by,

$$\left(n \frac{\partial I_{ijk}^{hs}}{\partial n_i} \right) = \sum_{l=0}^6 J_{l,K} \left(\frac{3b}{2\pi v} \right)^{l-1} \left(\frac{3}{2\pi v} \left[2 \sum_j x_j b_{ij} - \sum_i \sum_j x_i x_j b_{ij} \right] \right), \quad (A.14)$$

where n is the total number of moles of all the components in the phase, n_i is the number of moles of component i .

Appendix B. Supplementary data

Supplementary data associated with this article can be found, in the online version, at [doi:10.1016/j.gca.2006.05.007](https://doi.org/10.1016/j.gca.2006.05.007).

References

Anderko, A., Pitzer, K.S., 1991. Equation of state for pure fluids and mixtures based on a truncated virial expansion. *AIChE* **37**, 1379–1391.

- Anderko, A., Pitzer, K.S., 1993a. Equation-of-state representation of phase-equilibria and volumetric properties of the system NaCl-H₂O above 573-K. *Geochim. Cosmochim. Acta* **57**, 1657–1680.
- Anderko, A., Pitzer, K.S., 1993b. Phase equilibria and volumetric properties of the systems KCl-H₂O and NaCl-KCl-H₂O above 573 K—equation of state representation. *Geochim. Cosmochim. Acta* **57**, 4885–4897.
- Aranovich, L.Y., Newton, R.C., 1997. H₂O activity in concentrated KCl and KCl-NaCl solutions at high temperatures and pressures measured by the brucite-periclase equilibrium. *Contrib. Mineral. Petr.* **127**, 261–271.
- Aranovich, L.Y., Newton, R.C., 1998. Reversed determination of the reaction: Phlogopite + quartz = enstatite + potassium - feldspar + H₂O in the ranges 750–875 °C and 2–12 kbar at low H₂O activity with concentrated KCl solutions. *Am. Mineral.* **83**, 193–204.
- Bischoff, J.L., Pitzer, K.S., 1985. Phase relations and adiabats in boiling seafloor geothermal systems. *Earth Planet. Sci. Lett.* **75**, 327–338.
- Bischoff, J.L., Rosenbauer, R.J., Fournier, R.O., 1996. The generation of HCl in the system CaCl₂-H₂O: vapor-liquid relations from 380°C–500 °C. *Geochim. Cosmochim. Acta* **60**, 7–16.
- Boublik, T., 1970. Hard-sphere equation of state. *J. Chem. Phys.* **53**, 471–472.
- Brimhall, G.H., Crerar, D.A., 1987. Ore fluids: magmatic to supergene. In: Carmichael, I.S.E., Eugster, H.P. (Eds.), *Review in Mineralogy, Thermodynamic Modeling of Geological Materials: Minerals, Fluids and Melts*, vol. 17. Mineralogical Society of America, pp. 235–321.
- Bryan, P.F., Prausnitz, J.M., 1987. Thermodynamic properties of polar fluids from a perturbed-dipolar-hard-sphere equation of state. *Fluid Phase Equilib.* **38**, 201–216.
- Carmichael, I., Eugster, H., 1987. Thermodynamic modeling of geological materials: minerals, fluids and melts. In: Ribbe, P.H. (Ed.), *Reviews in Mineralogy*, vol. 17. Mineralogical Society of America, p. 499.
- Carnahan, N.F., Starling, K.E., 1969. Equation of state for nonattracting rigid spheres. *J. Chem. Phys.* **51**, 635–636.
- Chapman, W.G., Gubbins, K.E., Joslin, C.G., Gray, C.G., 1987. Mixtures of polar and associating molecules. *Pure Appl. Chem.* **59**, 53–60.
- Chase, M.W., Davis, C.V., Downey, J.R., Frurip, J.D., 1986. *JANAF Thermodynamical Tables*. ACS.
- Crovetto, R., Lvov, S.N., Wood, R.H., 1993. Vapor pressures and densities of NaCl(aq) and KCl(aq) at the temperature 623-K and CaCl₂(aq) at the temperatures 623-K and 643-K. *J. Chem. Thermodyn.* **25**, 127–138.
- Dimitrelis, d., Prausnitz, J., 1986. Comparison of two hard-sphere reference systems for perturbation theories for mixtures. *Fluid Phase Equilib.* **31**, 1–21.
- Dohrn, R., Prausnitz, J.M., 1990. A Simple perturbation term for the Carnahan-Starling equation of state. *Fluid Phase Equilib.* **61**, 53–69.
- Duan, Z., Moller, N., Weare, J.H., 1992. An equation of state for the methane-carbon dioxide-water system: II. Mixtures from 50 to 1000 C and 0 to 1000 bar. *Geochim. Cosmochim. Acta* **56**, 2619–2631.
- Duan, Z.H., Moller, N., Weare, J.H., 1995. Equation of state for the NaCl-H₂O-CO₂ system: prediction of phase equilibria and volumetric properties. *Geochim. Cosmochim. Acta* **59**, 2869–2882.
- Duan, Z.H., Moller, N., Weare, J.H., 2003. Equations of state for the NaCl-H₂O-CH₄ system and the NaCl-H₂O-CO₂-CH₄ system: phase equilibria and volumetric properties above 573 K. *Geochim. Cosmochim. Acta* **67**, 671–680.
- Fournier, R.O., 1987. Conceptual models of brine evolution in magmatic-hydrothermal systems. In: Decker, R.W., Wright, T.L., Stauffer, P.H. (Eds.), *Volcanism in Hawaii*. U.S. Geological Survey, NY, pp. 1487–1506.
- Frantz, J.D., Marshall, W.L., 1982. Electrical conductances and ionization constants of calcium chloride and magnesium chloride in aqueous solutions at temperatures up to 600C and pressures to 4000 bars. *Amer. J. Sci.* **282**, 1666–1693.
- Frantz, J.D., Popp, R.K., Hoering, T.C., 1992. The compositional limits of fluid immiscibility in the system H₂O-NaCl-CO₂ as determined with the use of synthetic fluid inclusions in conjunction with mass spectrometry. *Chem. Geol.* **98**, 237–255.
- Frape, S.K., Fritz, P., 1987. Geochemical trends for groundwaters from the Canadian Shield. In: Fritz, P., Frape, S.K. (Eds.), *Saline Water and Gases in Crystalline Rocks*, vol. 33. Geol. Assoc. Canada Spec. Pap, pp. 19–38.

- Gates, J.A., Wood, R.H., 1989. Density and apparent molar volume of aqueous $CaCl_2$ at 323–600 K. *J. Chem. Eng. Data* **34**, 53–56.
- Gubbins, K.E., 1985. Theory and computer-simulation studies of liquid-mixtures. *Fluid Phase Equilib.* **20**, 1–25.
- Gubbins, K.E., Twu, C.H., 1978. Thermodynamics of polyatomic fluid mixtures .1. Theory. *Chem. Eng. Sci.* **33**, 863–878.
- Gunter, W.D., Eugster, H.P., 1978. Wollastonite solubility and free-energy of supercritical aqueous $CaCl_2$. *Contributions to mineralogy and petrology* **66**, 271–281.
- Hass, J.L., 1971. The effect of salinity on the maximum thermal gradient of a hydrothermal system at hydrostatic pressure. *Econ. Geol.* **66**, 940–946.
- Hauzenberger, C.A., Baumgartner, L.P., Pak, T.M., 2001. Experimental study on the solubility of the “model-pelite mineral assemblage albite plus K-feldspar plus andalusite plus quartz in supercritical chloride-rich aqueous solutions at 0.2 GPa and 600 °C. *Geochim. Cosmochim. Acta* **65**, 4493–4507.
- Henley, R.W., Truesdell, A.H., Barton, P.B., Whitney, J.A., 1984. Fluid–mineral equilibria in hydrothermal systems. In: *Reviews in Economic Geology*, vol. 1. Society of Economic Geologists.
- Holmes, H.F., Busey, R.H., Simonson, J.M., Mesmer, R.E., 1994. $CaCl_2$ (aq) at elevated temperatures—enthalpies of dilution, isopiestic molalities, and thermodynamic properties. *J. Chem. Thermodyn.* **26**, 271–298.
- Janz, G.J., Tomkins, C.B., Allen, C.B., Downey, J.R., Gardner, J.L., Krebs, U., Singer, S.K., 1975. Molten salts: chloride and mixtures. *J. Phys. Chem. Ref. Data* **4**, 871–882.
- Jiang, S.Y., Pitzer, K.S., 1995. Thermodynamic properties of mixtures of dipolar and quadrupolar hard spheres—theory and simulation. *Journal of Chemical Physics* **102**, 7632–7640.
- Jiang, S.Y., Pitzer, K.S., 1996. Phase equilibria and volumetric properties of aqueous $CaCl_2$ by an equation of state. *AIChE Journal* **42**, 585–594.
- Ketsko, V.A., Urusova, M.A., Valyashko, V.M., 1984. Solubility and vapor pressures of solutions in the $CaCl_2$ system at 250–400 °C. *Russian J. Inorg. Chem.* **29**, 1398–1399.
- Larsen, B., Rasaiah, J.C., Stell, G., 1977. Thermodynamic perturbation-theory for multipolar and ionic liquids. *Molecular Physics* **33**, 987–1027.
- Mansoori, G.A., Carnahan, K.E., Starling, K.E., Leland, T.W., 1971. Equilibrium thermodynamic properties of the mixture of hard spheres. *J. Chem. Phys.* **54**, 1523–1525.
- Newton, R.C., 1995. Simple-system mineral reactions and high-grade metamorphic fluids. *European Journal of Mineralogy* **7**, 861–881.
- Newton, R.C., Aranovich, L.Y., Hansen, E.C., Vandenheuveel, B.A., 1998. Hypersaline fluids in Precambrian deep-crustal metamorphism. *Precambrian Research* **91**, 41–63.
- Oakes, C.S., Simonson, J.M., Bodnar, R.J., 1995. Apparent molar volumes of aqueous calcium chloride to 250 °C, 400 Bars, and from molalities of 0.242 to 6.150. *Journal of Solution Chemistry* **24**, 897–916.
- Obsil, M., Majer, V., Hefter, G.T., Hynek, V., 1997. Volumes of $MgCl_2$ (aq) at temperatures from 298 K to 623 K and pressures up to 30 MPa. *Journal of Chemical Thermodynamics* **29**, 575–593.
- Pak, T.M., Hauzenberger, C.A., Baumgartner, L.P., 2003. Solubility of the assemblage albite plus K-feldspar plus andalusite plus quartz in supercritical aqueous chloride solutions at 650 °C and 2 kbar. *Chemical Geology* **200**, 377–393.
- Pepinov, R.I., Lobkova, N.V., Zokhrabekova, G.Y., 1992. Density of water solutions of magnesium chloride and magnesium sulfate at high temperatures and pressures. *High Temperature-USSR* **30**, 66–70.
- Pitzer, K.S., 1973. Thermodynamics of electrolytes I. Theoretical basis and general equations. *J. Phys. Chem.* **77**, 268–277.
- Pitzer, K.S., 1987. Thermodynamic model for aqueous solutions of liquid-like densities. In: Carmichael, I.S.E., Eugster, H.P. (Eds.), *Reviews in Mineralogy—Thermodynamic Modeling of Geological Materials: Minerals Fluids and Melts*, vol. 17. Mineralogical Society of America, p. 499.
- Pitzer, K.S., Oakes, C.S., 1994. Thermodynamics of Calcium Chloride in Concentrated Aqueous Solutions and in Crystals. *Journal of Chemical and Engineering Data* **39**, 553–559.
- Pople, J.A., 1954. The statistical mechanics of assemblies of axially symmetric molecules. II. second virial coefficients. *Proc. of the Roy. Soc. A* **221**, 508–516.
- Rittner, E.S., 1951. Binding energy and dipole moment of alkali halide molecules. *J. Chem. Phys.* **19**, 1030–1039.
- Rushbrooke, G.S., Stell, G., Hoye, J.S., 1973. Theory of polar liquids. *Molecular Physics* **26**, 1199–1215.
- Shmulovich, K.I., Tkachemko, S.I., Plyasunova, N.V., 1995. Phase equilibria in fluid systems at high pressures and temperatures. In: Shmulovich, K.I. (Ed.), *Fluids in the crust: equilibrium and transport properties*. Chapman and Hall, pp. 193–214.
- Shvartsev, S.L., Bukaty, M.B., 1995. Evolution of $CaCl_2$ brine of Tungusky Basin (Siberian Platform): the role of water–rock interaction. In: *Proceedings of 8th International Symposium Water–Rock Interaction*, 477–481.
- Span, R., Wagner, W., 1996. A new equation of state for carbon dioxide covering the fluid region from the triple-point temperature to 1100 K up to 800 MPa. *J. Phys. Chem. Ref. Data* **25**, 1509–1596.
- Stell, G., Rasaiah, J.C., Narang, H., 1972. Thermodynamic perturbation theory for simple polar fluids, I. *J. Mole. Phys.* **23**, 393–406.
- Stell, G., Rasaiah, J.C., Narang, H., 1974. Thermodynamic perturbation theory for simple polar fluids, II. *J. Mol. Phys.* **27**, 1393–1414.
- Stephanopoulos, M.F., Gubbins, K.E., Gray, C.C., 1975. Thermodynamics of mixtures of non-spherical molecules II. strong polar, quadrupolar, and overlap forces. *Mole. Phys.* **30**, 1649–1676.
- Twu, C.H., Gubbins, K.E., 1978. Thermodynamics of polyatomic fluid mixtures. 2. polar, quadrupolar and octopolar molecules. *Chem. Eng. Sci.* **33**, 879–887.
- Twu, C.H., Gubbins, K.E., Gray, C.C., 1975. Excess thermodynamic properties for liquid mixtures of non-spherical molecules. *Mole. Phys.* **29**, 713–729.
- Urusova, M.A., Valyashko, V.M., 1983. Solubility, vapor-pressure and thermodynamic properties of solutions in the $MgCl_2$ - H_2O system at 300 to 350 °C. *Zhurnal Neorganicheskoi Khimii* **28** (7), 1845–1849.
- Urusova, M.A., Valyashko, V.M., 1984. Vapor-pressure and thermodynamic properties of magnesium–chloride aqueous-solutions at 250 °C. *Zhurnal Neorganicheskoi Khimii* **29** (9), 2437–2439.
- Wagner, W., Pruß, A., 2002. The IAPWS formulation 1995 for the thermodynamic properties of ordinary water substance for general and scientific use. *J. Phys. Chem. Ref. Data* **31**, 387–535.
- Wang, P., Oakes, C.S., Pitzer, K.S., 1998a. Thermodynamics of the system $MgCl_2$ - $NaCl$ - H_2O to 573 K: new measurements of heat of mixing and heat of dilution. *Int. J. Thermophys.* **19**, 739–748.
- Wang, P.M., Pitzer, K.S., Simonson, J.M., 1998b. Thermodynamic properties of aqueous magnesium chloride solutions from 250 to 600 K and to 100 MPa. *J. Phys. Chem. Ref. Data* **27**, 971–991.
- Weare, J.H., 1987. Models of mineral solubility in concentrated brines with application to field observations. In: Carmichael, I.S.E., Eugster, H.P. (Eds.), *Thermodynamic Modeling of Geological Materials: Minerals, Fluids and Melts*, vol. 17. Mineralogical Society of America, pp. 143–174.
- White, D.E., Hem, J.D., Waring, G.A., 1963. Chemical Composition of Subsurface Waters. In: Fleischer, M. (Ed.), *Data of Geochemistry*, vol. Chapter F, pp. 1–67. GPO.
- Winkelmann, J., 1981. Perturbation-theory of dipolar hard-spheres—the vapor–liquid equilibrium of strongly polar substances. *Fluid Phase Equilib.* **7**, 207–217.
- Winkelmann, J., 1983. Perturbation-theory of dipolar hard-spheres—the vapor–liquid equilibrium of strongly polar mixtures. *Fluid Phase Equilib.* **11**, 207–224.
- Wood, S.A., Crerar, D.A., Brantley, S.L., Borcsik, M., 1984. Mean molal stoichiometric activity coefficients of alkali halides and related electrolytes in hydrothermal solutions. *Amer. J. Sci.* **284**, 668–705.
- Zarembo, V.I., L’vov, S.N., Matuzenko, J., 1980. Saturated vapor pressure of water and activity coefficients of calcium chloride in the $CaCl_2$ - H_2O system at 423–623 K. *Geochem. Intl.* **4**, 159–162.
- Zhang, Y.G., Frantz, J.D., 1989. Experimental determination of compositional limits of immiscibility in the $CaCl_2$ - H_2O - CO_2 system under high temperatures and pressures using synthetic fluid inclusions. *Chem. Geol.* **74**, 289–308.